Lead-Bismuth Target Design for Transmutation Reactors

Yousry Gohar, Phillip Finck, Joseph Herceg, Lubomir Krajtl, W. David Pointer, James Saiveau, Tanju Sofu
Argonne National Laboratory, Argonne, IL 60439, USA
gohar@anl.gov, pfinck@anl.gov>, jeherceg@anl.gov, lkrajtl@anl.gov>, dpointer@anl.gov, saiveau@anl.gov, tsofu@anl.gov

Albert Hanson, and Michael Todosow
Brookhaven National Laboratory, Upton, NY 11973, USA
alh@bnl.gov, todosowm@bnl.gov

Maria Koploy, Panto Mijatovic,
General Atomics, San Diego, Ca 92121, USA
maria.koploy@gat.com, panto.mijatovic@gat.com

ABSTRACT

A lead-bismuth eutectic (LBE) target design has been developed to drive the subcritical multiplier (SCM) of the accelerator-driven test facility (ADTF). This paper gives the target design description, the main results from the parametric studies, and the design analysis including physics, heat-transfer, hydraulics, structure, activation, and decay heat removal analyses. The design is based on a coaxial geometrical configuration to minimize the target footprint since the target is installed vertically along the SCM axis. LBE is the target material and the target coolant. Ferritic steel (HT-9 alloy) is the selected structural material based on the current database and the design analyses. A uniform proton beam is employed to perform the spallation process. The proton beam current is 8.33-mA and the current density is 40-$\mu A/cm^2$, which requires a beam radius of 8.14-cm. The beam power is 5 MW and the proton energy is 600 MeV. The beam tube has 10-cm radius to accommodate the halo current. A hemi-spherical geometry is used for the target window, which is connected to the beam tube. The beam tube is enclosed inside two coaxial tubes to provide inlet and outlet channels for the LBE coolant. The coolant channels and the proton beam enter vertically from the top above the SCM. Several design constrains are defined and utilized for the target design process to satisfy different engineering requirements and to minimize the design development time and cost.

1. INTRODUCTION

A spallation target design [1] has been developed to provide the required neutron source for the subcritical multiplier (SCM) of the accelerator driven test facility (ADTF). The ADTF is a major nuclear research facility that will provide multiple testing and production capabilities. The main ADTF mission includes the capability to assess technology options for the transmutation of spent nuclear fuel and nuclear waste through proof-of-performance demonstrations; the ability to operate as a user facility that allows testing advanced nuclear technologies and applications, material science and research, experimental physics, and conventional nuclear engineering science applications; and the capability, through upgrades to produce radioisotopes for medical and commercial purposes. Multiple target stations are envisioned to accommodate the mission. The principal target station consists of a spallation target and a subcritical multiplier (SCM) with a power rating up to 100 MW. This SCM will provide the prototypic environment necessary to support the transmutation proof of performance. In addition, a target and material test station will be used to test a wide range of target designs, fuel assemblies, and coolants for developing components for the SCM. The work presented in this paper is intended to cover the analyses and the design of the SCM lead-bismuth target.

The spallation target design is based on a coaxial geometrical configuration to satisfy the SCM configuration for minimizing the space requirements and to maximize the SCM utilization of the target neutrons. The target is installed vertically along the SCM axis. Lead-Bismuth Eutectic (LBE) is the target material and the target coolant. Ferritic steel (HT-9 alloy) is the selected structural material for the target based on the current database and the design analyses. Austenitic steel (Type 316 stainless steel) is the second choice. A uniform proton beam is employed to perform the spallation process. The beam power is 5 MW and the proton energy is 600 MeV. The coolant channels and the proton beam are entered vertically from the top above the SCM. The LBE flow cross-section area is maintained at a constant value along the axial direction to maintain a constant average coolant velocity, which improves the target hydraulic design. The geometrical configuration has been carefully designed to ensure flow stability and adequate cooling of the beam window and the structural material. Target design objectives were defined to guide the design process. Design constraints are determined and used in the target design process to satisfy different engineering requirements, to minimize the design development time and cost, to ensure a satisfactory operating performance, and to maximize the operating lifetime of the target structural material.

Physics analyses were performed using the Monte Carlo code MCNPX [2] to account for the geometrical details, the spallation process, and the production and the transport of the spallation products. Parametric analyses were performed to study the neutron yield, the neutron source spectrum, the energy deposition distribution, the buffer size between the target and the subcritical multiplier, and the nuclear responses. Also, the neutronic performance of the SCM with MK-III EBR-II fuel (driver fuel) was analyzed with the target design to define the SCM neutron flux and the energy deposition distribution in the system. The fast neutron flux is a key operating parameter for testing nuclear fuels and demonstrating the transmuter proof-of-performance.

Thermal hydraulic analyses were carried out to define the velocity distribution and the flow stability of the lead-bismuth eutectic and the temperature distribution in the target structure and the target coolant. Also, the hydraulic results were used to update the geometrical configuration and to improve the coolant flow stability. Parametric analyses were performed and iterated with the other design analyses to define the reference design.

Structural analyses were executed parametrically in conjunction with the thermal hydraulic analyses to check the design compliance with the stress and buckling design criteria developed for the Accelerator Production of Tritium project [3] and the International Thermonuclear Experimental Reactor [4] for irradiated structural materials. Also, the results are used to select the shape and thickness of the beam window to maximize the engineering design margins.

Activation analyses were done to define the inventory of the radioactive isotopes as a function of the operating time and the decay time after shutdown. These isotopes define the radiological toxicity and the decay heat source from the lead-bismuth target material as a function of the decay time after shutdown. The design analyses utilize the decay heat source to check the maximum temperature during abnormal conditions with respect to the maximum allowed temperature for the structural material. Also, the dose rate from the gamma rays of the generated radioactive isotopes was calculated to define the required input for calculating the appropriate time schedule and the shielding requirements for maintaining the target system.

This paper describes the different studies and the obtained results as well as the reference target design. The target design and the performance parameters of the subcritical multiplier are defined based on the obtained results.

2. DESIGN OBJECTIVES AND CONSTRAINTS

The main objective of the target design is to generate the required neutron source to drive the SCM. The neutrons are generated from the LBE spallation reactions driven by the 600-MeV proton beam and the neutron multiplication reactions of the high-energy spallation neutrons with the LBE. The beam power is 5 MW and it has a uniform spatial distribution over the beam cross-section area. The SCM design requires a small target diameter to simplify the SCM design and the target replacement procedure, to reduce the neutron losses in the axial direction, to decrease the shield volume, and to reduce the number of the SCM fuel assemblies required for achieving the 100 MW power level. However, the structural material and the heat transfer considerations require a large beam diameter to reduce the energy deposition and the irradiation damage densities in the beam window. The other main objectives for the target design are to protect the SCM from the high-energy protons and neutrons, to contain the spallation products, to help achieving the availability goal of the facility, and to reduce the shutdown time for target replacement during normal and abnormal conditions. Also, the target has to generate a uniform neutron source along the beam axis as much as possible to minimize the SCM axial power peaking.

Operating constrains are imposed on the target design to satisfy different engineering requirements and to minimize the design development time and cost. Existing structural materials, ferritic steel (HT-9) and austenitic steel (Type 316SS) are the selected structural materials for the target design. LBE is used as a target material and coolant to simplify the design. The surface temperature of the structural material in contact with the LBE is limited to less than 550 C to reduce erosion and corrosion concerns. This temperature limit assumes that the coolant chemistry is controlled to maintain an oxide layer on the structural material surface for corrosion protection. The stress analysis of the irradiated structural materials limits the maximum temperature to less than 550 and 600 ºC for HT-9 and Type 316SS, respectively, for maintaining adequate mechanical properties. The average coolant velocity is limited to ~2 m/s based on the current database to reduce erosion and corrosion concerns. The coolant pressure is minimized to avoid high primary stresses in the structural material. The coolant inlet temperature is 200 ºC, which provides adequate design margin above the LBE melting point of 129 ºC. The outlet temperature is constrained by the maximum allowable temperature for the structural material. Heat conduction to the back shine shield in the beam tube, natural convection, and radiation to the sodium pool are used to remove the decay heat from the target material. These objectives and constraints are utilized to develop the current LBE target design presented in this paper.

3. DESIGN DESCRIPTION

The proton beam has a total current of 8.33 mA distributed uniformly over a circular cross section. The beam current density is 40 $\mu A/cm^2$ and the corresponding beam radius is 8.14 cm. The beam tube has 10-cm radius to accommodate the halo current. A hemi-spherical geometry is used for the beam window, which is connected to the beam tube. A conical window with a rounded tip is also considered since it has a lower average temperature relative to the hemi-spherical geometry. The beam tube is enclosed inside two coaxial tubes to provide inlet and outlet channels for the LBE coolant. The double function of the LBE as a target material and target coolant does simplify the design. The radii of these tubes were adjusted to achieve the same average coolant velocity in the inlet and the outlet channels. The outer channel is used for the inlet flow to improve the coolability of the beam window. The edge of the inside tube between the inlet and the outlet flow is terminated with a rounded fairing to improve the flow stability. The fairing configuration was carefully designed and it is tangent to the inlet side surface of the middle wall and extends into the outlet flow field. The geometrical details of the target design are shown in Figure 1. A guard tube is used to enclose the target design. It provides a confined space to check and contain any leakage. Also, this space provides a buffer between the SCM sodium pool and the LBE. Helium gas at low pressure is used to fill the space. HT-9 is the selected structural material and Type 316SS is the backup. The LBE oxygen concentration is maintained in the range of 10^{-6} to 10^{-4} at% to reduce corrosion concerns.

The beam tube enters the subcritical multiplier building horizontally, and then the beam is bended 90º to reach the subcritical multiplier. The vertical section of the beam tube is ~14.1 m after the last bending magnet. The coolant channels have a vertical length of about 10.1 m before changing direction to connect horizontally with the external section of the LBE loop. Pressurized helium gas is used to heat the target structure before the target is filled with the LBE. Also, helium is utilized to drain the LBE using a small vertical tube(s) of ~1-cm diameter, which reaches the target bottom section. In the target replacement procedure, the LBE is drained before the target tubes are disconnected for removal. A crane is used to pull the empty target structure inside the target replacement cask.

Inside the guard tube, chemical and pressure sensors are used to check for Na or LBE leakage. These sensors provides early warning to avoid the possibility of mixing the two fluids, which reduces the maintenance down time and improves the safety performance. The beam tube vacuum is also monitored to detect any LBE leakage through the beam tube.

4. PHYSICS DESIGN

Detailed MCNPX models were developed that include the target, the SCM, and the sodium pool to perform target, buffer, parametric, and SCM design analyses. Mark-III EBR-II fuel is used for the SCM. In these models, the spallation products were transported and the nuclear responses were tallied. The fuel loading was adjusted to achieve a total system power of 100 MW with the 5 MW beam power.

The physics analysis defined the required target length to stop the proton beam and the axial energy deposition profile. Figure 2 shows the energy deposition profile as a function of the distance alone the beam axis with 0.5-cm thick steel window. The required target material length is ~32 cm to stop the 600-MeV protons. The peak energy deposition is 796 W/cm^3 at 1.75 cm from the LBE surface for the uniform current density of 40 $\mu A/cm^2$. Table 1 gives the nuclear responses in the target window for iron, which represent a good simulation for the HT-9 alloy. In the beam window, the neutrons are responsible for 69% of the atomic displacement and the protons are generating more than 96% of the gas production rate.

The MCNPX models were used to define the target buffer size taking into consideration the total neutron yield from the target, the spallation neutron fraction utilized by the subcritical multiplier, and the nuclear responses in the structural material next to the target. The analysis was performed as a function of the buffer thickness. The cross section area required for the inlet and the outlet channels define the minimum buffer thickness, which is 7 cm. The results show that the number of spallation neutrons per proton has low sensitivity to the buffer thickness as shown in Figure 3. It reaches a saturation value at a buffer thickness of ~40 cm. The saturation value is about 1.14 times the value obtained with the 7 - cm minimum buffer thickness. However, the number of spallation neutrons reaching the subcritical multiplier is significantly reduced as the buffer thickness is increased. This is shown in Figure 3 where this number drops from 7.8 neutrons per proton with 7-cm buffer to ~3.3 neutrons per proton with 40-cm buffer. The axial neutron leakage is increased as the buffer thickness is increased. This requires the target design to reduce the buffer thickness as much as possible.

For a small buffer thickness, the nuclear responses in the structural material outside the buffer peaks near the SCM midplane. As the buffer thickness increases, the peak values of the gas production, helium and hydrogen, shift to the top section of the SCM. On the other hand, the maximum atomic displacement stays at the SCM midplane. For a constant system

power, as the buffer thickness increases, the SCM volume increases to compensate for the increased neutron leakage. Therefore, the SCM average power density and the nuclear responses are decreased. The nuclear responses at the SCM midplane are shown as a function of the reciprocal of the outer buffer radius in Figure 4. The results show a good linear fit because the fission neutrons dominate the reaction rates at the SCM boundary. The other important parameter for the structural material performance is the helium to atomic displacement ratio. Figure 5 shows this ratio as a function of the buffer thickness, which is in the range of 0.1 to 0.3. This ratio is ~0.26 for HT-9 in a typical fast fission reactor spectrum. These results show that the 7-cm buffer thickness protects the structural material from the high energy neutrons (E> 20 MeV), utilizes most of the spallation neutrons for driving the subcritical multiplier, and provides adequate cross section area for the inlet and the outlet coolant channels.

The neutron source spectrum was calculated over the outer buffer surface because these neutrons drive the subcritical multiplier. The neutron spectrum peaks in the energy range of 0.6 to 0.7 MeV as shown in Figure 6. The high-energy tail extends all the way up to ~600 MeV. The neutron percentage with energy above 20 MeV entering the subcritical multiplier or leaking from the target top section is 6.4%. On the other hand, this percentage is 12.3 for the neutrons leaving the bottom target section, which shows the forward peaking of the high-energy neutrons.

The spatial distribution of the spallation neutrons in the axial direction has a direct impact on the axial power peaking in the subcritical multiplier. The axial distribution of the spallation neutrons peaks at ~12 cm from the upper surface of the lead-bismuth material while the high-energy neutrons (above 20 MeV) peak at ~14.5 cm as shown in Figure 7. The peak to the average ratio is 1.33 and the peak to the minimum ratio is 4.11. The impact on the power distribution of the subcritical multiplier is shown in the SCM performance section.

5. THERMAL HYDRAULIC DESIGN

Parametric thermal hydraulic analyses were performed to determine the temperature distribution in the target materials and the velocity distribution of the lead-bismuth eutectic as a function of the target design parameters. The results are used to select the target flow direction with respect to the beam window, to modify the target geometry for increasing the flow stability, and to select the target structural material. The peak structural temperature

was reduced as much as possible to satisfy the engineering design requirements. The inlet coolant conditions are set to ensure that the peak liquid-solid interface temperature is less than 550 ºC. Furthermore, the inlet conditions are set so that the average flow velocity is 2 m/s to reduce corrosion and erosion concerns in the target system. Two structural materials (Type 316SS and HT-9), two different inlet temperatures, two different flow paths with respect to the beam window, and geometrical variations were considered in the parametric analyses. Type 316SS structure exhibits more desirable machining and fabrication properties, however HT-9 exhibits more desirable corrosion resistance properties and higher thermal conductivity. In order to ensure that LBE remains liquid throughout the system, the minimum inlet temperature must be above 180 °C. An inlet temperature of 200 °C is considered for the target system. Since the inlet and the outlet channels of the target section use coaxial tubes, the inlet LBE will be heated before it reaches the target section. In the analyses, the inlet temperature for the target section is 220 °C to account for the heat transfer from the hot to the cold channel. The inlet and the outlet channels are reversed for some cases to examine the effect on the local heat transfer coefficients in the heated region. The study includes also a number of geometrical variations, changes in the inclination of the middle walls and the beam window geometry from hemi-spherical to conical.

The thermal hydraulic characteristics of the LBE target are dominated by three primary characteristics of the proposed target design. First, energy is deposited volumetrically in the bulk target region of the flow field. Second, the energy deposition rate in the solid structure within the beam window region is significant. Finally, a compact 180-degree turn in flow direction is needed to provide a return path to the outlet. These characteristics limit the applicability of existing analytical and empirical correlations for evaluating the temperature and the velocity profiles within the system. Therefore, the thermal hydraulic evaluations were performed with the commercially Computational Fluid Dynamics (CFD) software package STAR-CD [5].

The parametric study results provided crucial information needed to develop a target design that satisfies the design requirements. Cases with the flow enter the target area through the outer annulus and exits through the inner annulus show lower peak temperatures relative to the other cases. Cases with the middle wall angle increased provide small reduction in the beam window temperature distribution while the middle wall peak temperatures are significantly increased. For conical beam windows, changing the cone angle has little impact on the temperature distribution. The use of 220 °C inlet temperature is essential to

reduce the peak temperature in the target structure. A small difference is observed between the temperature distribution of the conical and the hemi-spherical beam windows. While the stagnation point at the centerline of the hemi-spherical beam window raises the temperatures in that region above those seen in the cone-shaped beam window, the remainder of the temperature distributions is nearly identical. The shape of the beam window can be altered as needed to meet mechanical and thermal stress requirements with little impact on the temperature distribution in the target. HT-9 cases show that a window wall thickness of 4.0 mm or less satisfies the temperature design requirements with 200 °C inlet temperature. In all the cases of the parametric study, the formation of a toroidal recirculation zone was predicted as the fluid turns around the middle wall. Standard flow control methodologies [6] are used for reducing the instability resulting from annular turn geometries. To increase the stability of the flow field in the target area, the middle was carefully modified so that its leading edge near the end cap terminates in a rounded fairing as shown in Figure 1.

Design iterations including thermal hydraulics, thermal stresses, and structural analyses were performed to define the target design. The selected configuration has a 3.5-mm hemi-spherical beam window with a 5-mm thick beam tube. The velocity and the temperature profiles for this beam tube are shown in Figure 8. The peak and the surface temperature limits are satisfied. The temperature distribution was utilized for the structural analyses for analyzing thermal and mechanical stresses in the beam tube. The outlet LBE temperature is approximately 280 ˚C for a target module inlet temperature of 200 ˚C. The total pressure drop through the target system is approximately 32 psi. The peak temperatures on the adiabatic and wetted surfaces of the beam window are 502 ˚C and 341 ˚C, respectively, which provide a substantial margin below the specified limits.

6. STRUCTURAL DESIGN

The ability of the beam tube, including the beam window, to withstand the mechanical loads, the thermal stresses, and the irradiation effects is determined by comparing the calculated stresses to allowable stresses defined in the APT supplemental structural design requirements [3], the international thermonuclear experimental reactor [4], and the ASME code. A stress analysis was performed for various beam tube configurations with different loading conditions and irradiation fluence values. The ANSYS general-purpose finite element code [7] was used with a two-dimensional axisymmetric finite element model for the beam tube. The LBE hydrostatic pressure load and the temperature gradient were included in the analysis.

The buckling capabilities of the beam tube were initially evaluated using the ASME code. Then, a nonlinear buckling analysis was performed using ANSYS code. The analysis was aimed to develop a beam tube configuration, which would satisfy the allowable stresses and the buckling criteria for the one-year lifetime goal.

A parametric stress analysis was performed to study the effect of the window wall thickness and the window geometry on the generated stresses. The window wall thickness was parametrically changed for the conical and hemi-spherical geometries. The mechanical load is the external pressure due to the hydraulic head from the liquid lead-bismuth eutectic in the target system. This pressure load is 0.79 MPa. The temperature distribution of the beam tube is obtained from the thermal hydraulic analysis. The mechanical properties are evaluated as a function of temperature and irradiation fluence. Based on the results from the parametric study and the allowable stresses for the HT-9 structure, a 3.5-mm window wall thickness was selected. A sample of the results is shown in Figure 9 for the hemi-spherical window. The peak stress occurs near the intersection of the proton beam boundary with the beam window. The peak stress values of the two geometries, hemi-spherical and conical are very close, which qualify both geometries for further considerations.

Unirradiated HT-9 has very low ductility, the minimum uniform elongation is ~2.5%. Therefore it is reasonable to assume that a small fluence will reduce the uniform elongation below 2%. The allowable HT-9 stresses were calculated assuming no ductility left due to irradiation effects. Fission and fusion HT-9 databases with neutron fluence up to 72 dpa were used for the analysis. These databases need to be confirmed for higher helium production expected during the operation. The calculated stresses for the 3.5 mm wall thickness for the conical and the hemi-spherical beam windows at the appropriate temperature for each stress component are given in Table 2. Also, the allowable stress for each stress component defined in the structural design rules [3,4] is given to compare with the calculated values. All the stress values are less than the allowable stresses except the (P_L+P_B+Q) stress component for the conical window geometry, which slightly exceeds the allowable stress (S_{d2}). Reducing the thickness to 3 mm instead of the 3.5 mm will satisfy this stress component for the conical window. The hemi-spherical window satisfies all allowable stresses.

Linear Buckling Analysis was carried out for the beam tube as a function of the wall thickness for the beam window and the cylindrical section. The analysis used the methods presented in Article D-3 of the ASME Code Section VIII, Division 2, Shells of Revolution

Under External Pressure [8]. The result shows that for Type 316SS, the wall thickness of the cylindrical section of the beam tube should be more than 4.5 mm to meet the ASME code. For the conical and hemi-spherical beam windows, the wall thicknesses have to exceed 2.5 and 1.6 mm, respectively. For the same window thickness, the hemi-spherical configuration has a larger buckling margin relative to the conical. In this evaluation, the radiation and temperature effects were not included.

Non-linear buckling analysis was carried out for the HT-9 beam tube with the hemi-spherical beam window. Based on the previous results, the thickness of the different sections of the beam tube was defined for this analysis to define the critical buckling load. The beam window thickness is 3.5 mm and the wall thickness of the cylindrical section is 5 mm. The finite element model used 4-node shell elements (ANSYS Shell 181). At the open end of the beam tube, the three translations are constrained and the normal operating temperature distribution is used. A uniform external pressure of 10 MPa was applied gradually during the solution process. Also, a small percentage of the first linear buckling mode shape is added to the model as an initial geometrical imperfection to obtain the critical buckling load. The influence of irradiation on the critical buckling load was evaluated by running the analysis with the unirradiated and irradiated HT-9. The results show that the beam tube configuration has a large safety margin against buckling for both unirradiated and irradiated HT-9. The critical load levels for those two cases are 5.64 and 5.74MPa, respectively, which are much higher than the working external pressure of 0.79 MPa. The total stress intensity due to the critical load of 5.74 MPa are shown in Figure 10 for the irradiated HT-9 with 25 dpa.

7. ACTIVATION ANALYSES AND DECAY HEAT REMOVAL

Activation analyses have been performed for the LBE target design of the ADTF. The analyses are based on the MCNPX model developed for the physics analyses, coupled with the ORIGEN2-S code for the evaluation of isotopic production/destruction and decay. The decay power from the LBE target material is compared to lead, bismuth, and LBE with vacuum boundary condition (without the SCM) to define the impact of the reflected neutrons from the SCM. Figure 11 shows a comparison of the buildup of radioisotope decay power as a function of irradiation time, up to one year. The geometrical model for the decay power of the target material includes the different components of the system: the fuel, the reflector, and the sodium pool. The difference between the power of the LBE target material and the

LBE cylindrical geometry on this figure is due to the particles and the photons entering the LBE target from the surroundings. The decay power of the radioactive isotopes after shutdown is plotted in Figure 12.

The target performance was evaluated during loss of flow event without the use of an active engineering system. Radiation heat transfer between the LBE inventory of the target and the sodium inventory of the surrounding SCM pool is used to calculate the LBE temperature as a function of time after shutdown. For this analysis, it is assumed that the proton beam is terminated at the onset of loss of flow conditions. The spatial dependence of the temperature within the LBE inventory and the sodium inventory is neglected. The conductive resistance of the target vessel walls and the guard vessel walls is neglected as well. However, radiation heat transfer properties of the steel vessel walls are used in the radiation calculation. The gap between the target vessel and guard vessel is treated as an idealized void with no conduction or radiative absorption. The sodium pool is assumed to be at a uniform temperature of 370 ºC and is treated as an infinite medium surrounding the target module. No credit is taken for natural convection within the LBE inventory. After approximately 8 days, the LBE inventory temperature reaches a peak value of approximately 752 ºC (1025 K) and begins to decrease. This peak temperature allows the target to re-operate without replacement [9]. In conclusion, the management of decay heat in the ADTF LBE target concept may not require an active engineering system for the decay heat removal.

8. SUBCRITICAL MULTIPLIER PERFORMANCE PARAMETERS

The MCNPX geometrical model of the lead-bismuth target design and the subcritical multiplier with the vertical proton beam was also used to define the neutron flux and the energy deposition distribution in the system. The model has EBR-II Mark-III driver fuel and 5 MW beam power. The fuel loading is adjusted through several iterations to provide a total power deposition of 100 MW in the target and the subcritical multiplier. Figure 13 shows the spatial distribution of the fast neutron flux in the target and the fuel zone for neutrons in the energy range of 0.1 to 20 MeV. The proton beam radius is ~8 cm and the buffer thickness is 7 cm. The inner and outer fuel zone radii are 15 and 25 cm, respectively. The peak fast flux is about 3 x 10^{15} n/cm^2/s. The spatial distribution of high-energy neutrons above 20 MeV has a peak value of 2 x 10^{13} n/cm^2/s in the fuel zone. The high-energy neutron flux is less than 1% of the total flux. The energy spatial deposition distribution is shown in Figure 14. The power distribution shows clear distinction between

the proton beam, the target buffer, and the fuel zone boundaries. The peak energy deposition in the fuel zone is 800 W/cm^3.

CONCLUSIONS

An LBE target design has been developed successfully for the SCM station of the ADTF. Target design objectives and constraints were defined and utilized to satisfy different engineering requirements and to minimize the design development time and cost. The ADTF mission and goals did define some of the objectives. Physics, heat-transfer, hydraulics, structure, activation, and safety analyses were iterated to develop the current target design.

ACKNOWLEDGEMENTS

The submitted manuscript has been created by the University of Chicago as Operator of Argonne National Laboratory ("Argonne") under contract No. W-31-109-ENG-38 with the U.S. Department of Energy. The U.S. Government retains for itself, and others acting on its behalf, a paid-up, nonexclusive, irrevocable worldwide license in said article to reproduce, prepare derivative works, distribute copies to the public, and perform publicly and display publicly, by or on behalf of the Government.

REFERENCES

1. Yousry Gohar, Phillip Finck, Albert Hanson, Joe Herceg, Maria Koploy, Lubomir Krajtl, Panto Mijatovic, W. David Pointer, James Saiveau, Tanju Sofu, and Michael Todosow, "Lead- Bismuth Target Design for the Subcritical Multiplier (SCM) of the Accelerator Driven Test Facility (ADTF)," Argonne National Laboratory Report, ANL/TD/02-01, 2002
2. L. S. Waters, Editor, MCNPX User's Manual – Version 2.1.5, TPO-E83-UG-X-00001, Revision 0, Los Alamos Report, November 14, 1999.
3. Supplemental Structural Design Requirements, PPO-P00-G-PRD-X-00006, Rev. A
4. S. Majumdar and P. Smith, Treatment of irradiation effects in structural design criteria for fusion reactors, Fusion Engineering and Design 41, 1998.
5. STAR-CD Version 3.1B, CD-Adapco Group.
6. I.E. Idelchik, Handbook of Hydraulic Resistance, 3rd ed., Boca Raton, FL: CRC Press, 1994.
7. ANSYS Version 5.7, ANSYS, Inc.,2000.
8. ASME Code Section VIII, Division 2, Article D-3; Shells of Revolution Under External Pressure.
9. D. Smith, W. Dänner, Y. Gohar et al., "ITER Blanket, Shield and Material Data Base - Part A (ITER Blanket and Shield)," International Atomic Energy Agency, Vienna, ITER Documentation Series, No. 29, 1991.

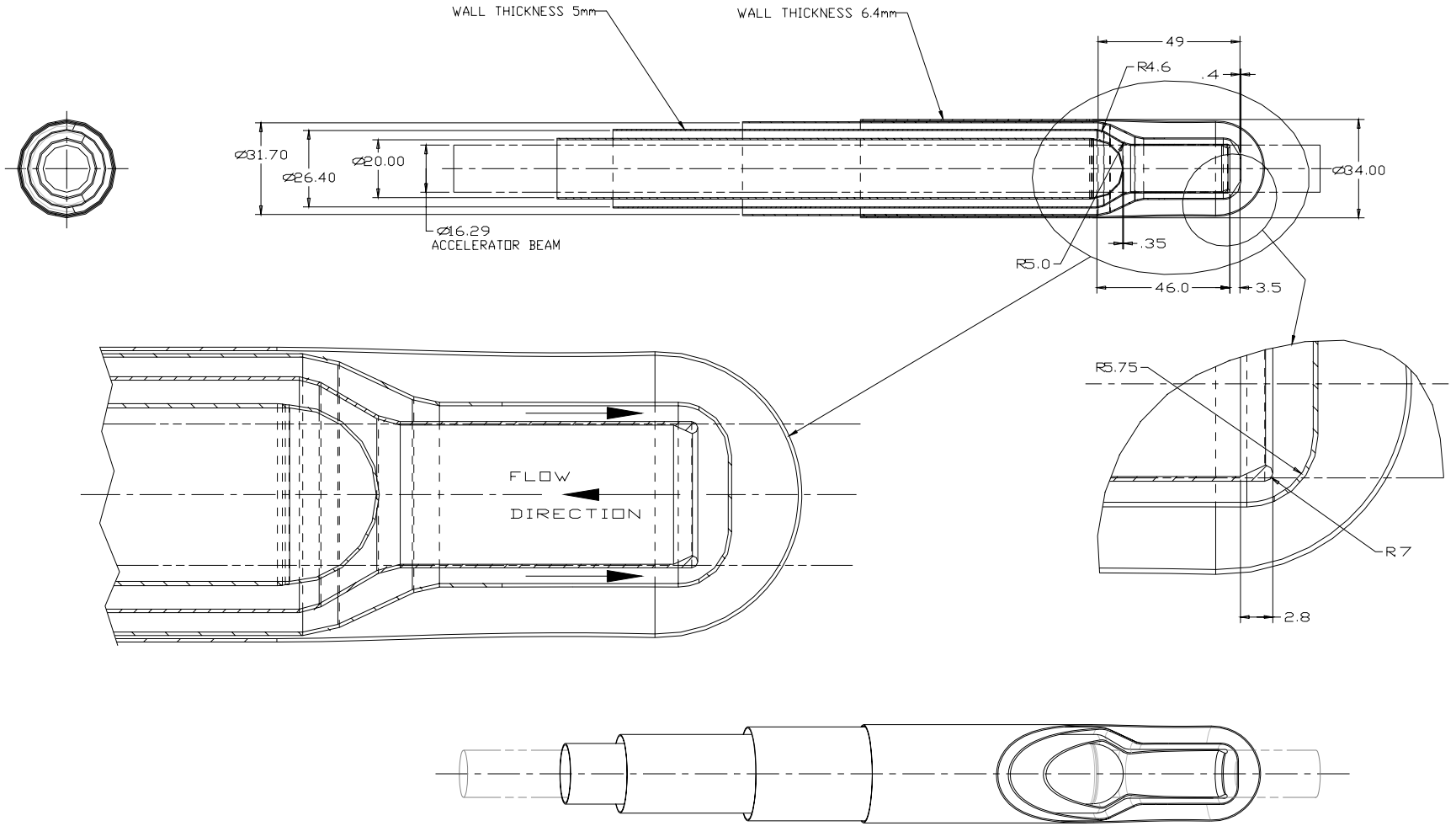

Figure 1. Lead-bismuth eutectic target design

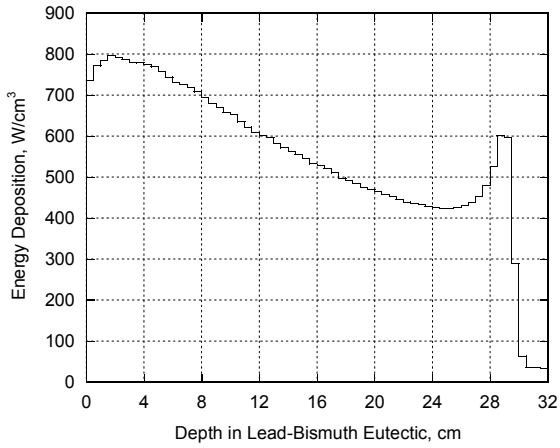

Figure 2. LBE axial energy deposition

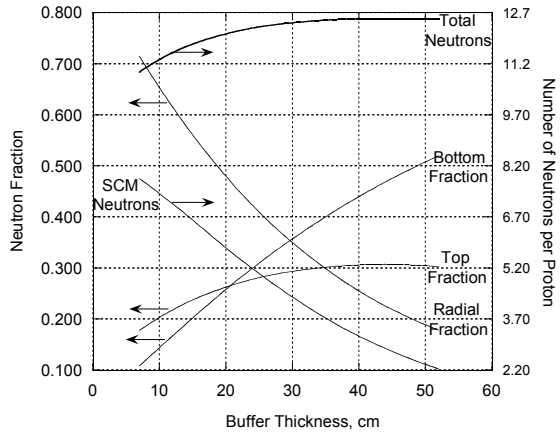

Figure 3. Neutron source yield as a function of the LBE buffer thickness

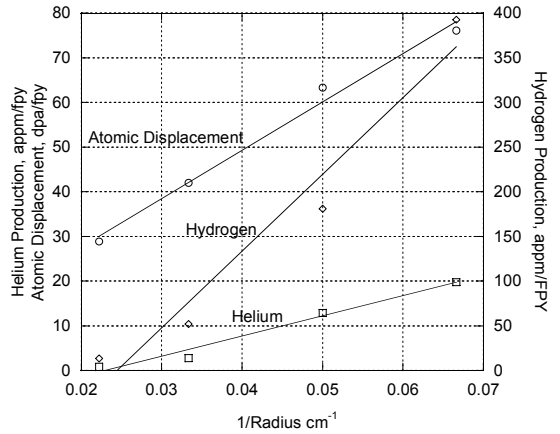

Figure 4. Midplane nuclear responses in the outer buffer structure as a function of the reciprocal of the LBE outer buffer radius

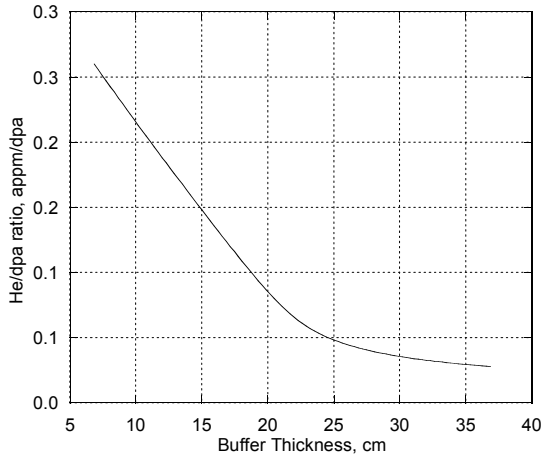

Figure 5. Helium/atomic displacement ratio as a function of the buffer thickness

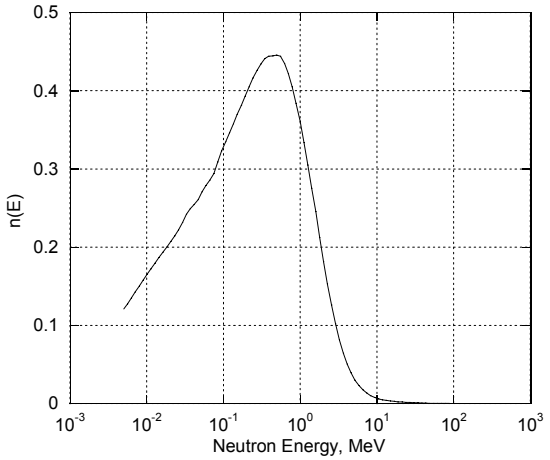

Figure 6. Neutron source spectrum

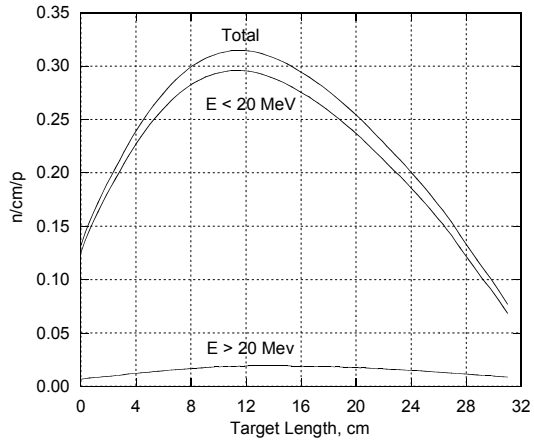

Figure 7. Neutron source distribution along the outer buffer surface

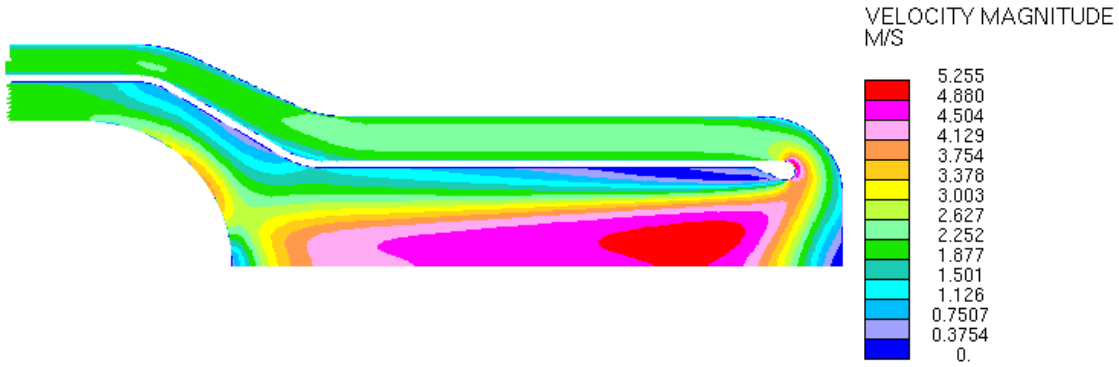

(a)

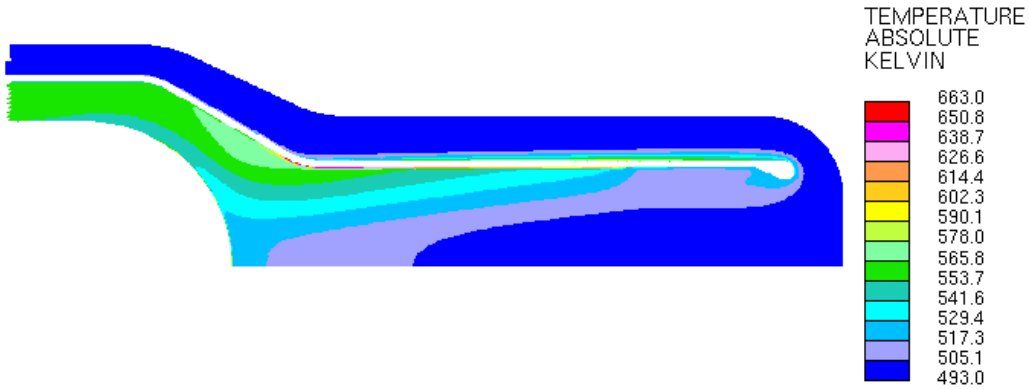

(b)

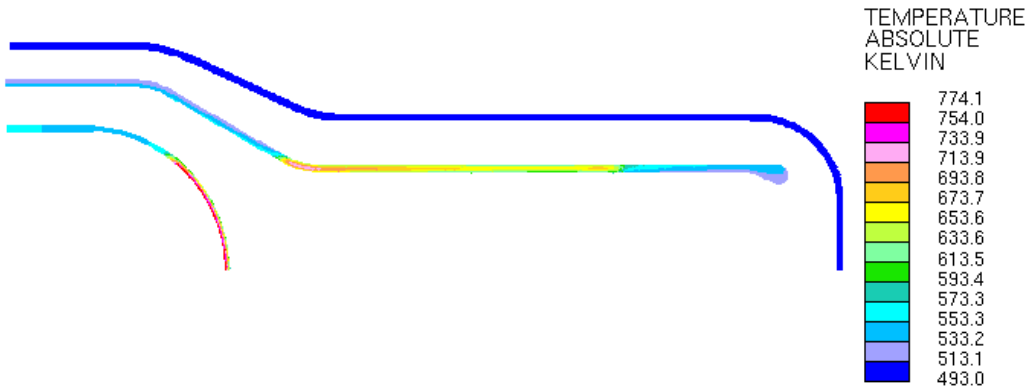

(c)

Figure 8. LBE target concept contour plots showing (a) fluid velocity, (b) fluid temperature, and (c) structural temperature profiles

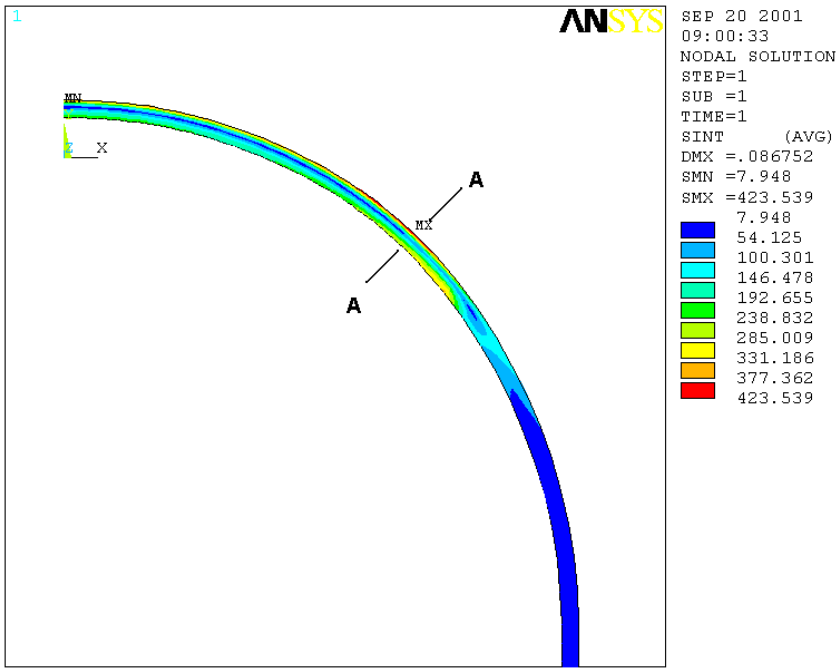

Figure 9. Stress intensity (Pa) in the 3.5-mm hemi-spherical beam window during the normal operating conditions

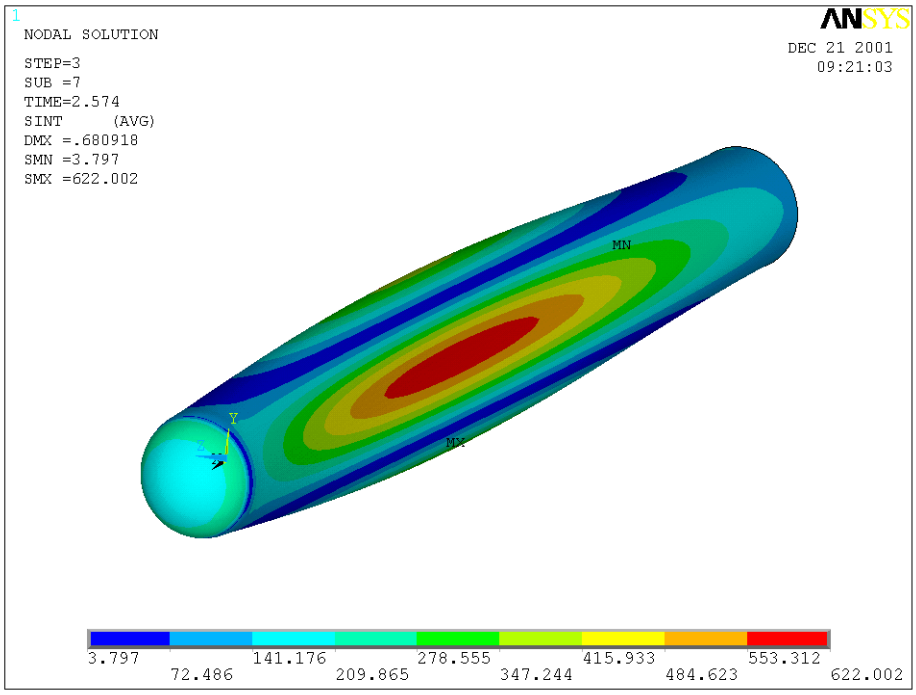

Figure 10. Total Stress Intensity (MPa) contour plot for external pressure of 5.74 MPa using irradiated HT-9 with 25 dpa

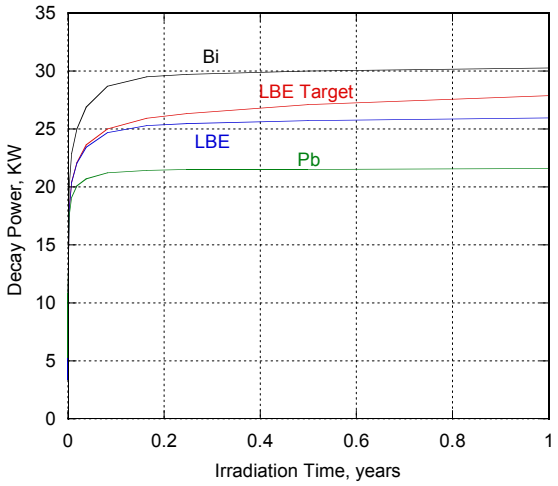

Figure 11. Buildup of decay power in a bismuth, lead, or LBE cylindrical geometry compared to LBE target material

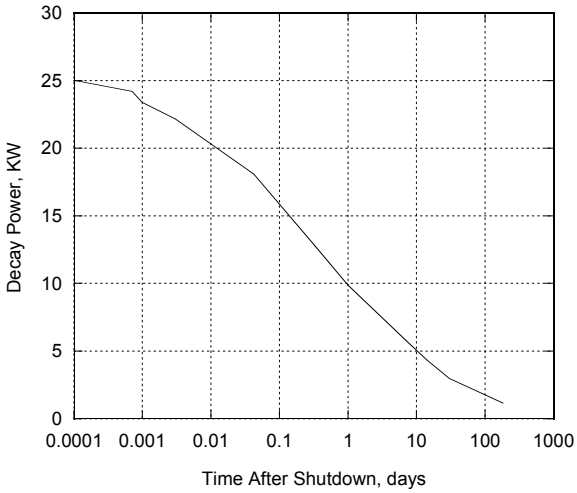

Figure 12. Decay power from the LBE target material as a function of time after shutdown

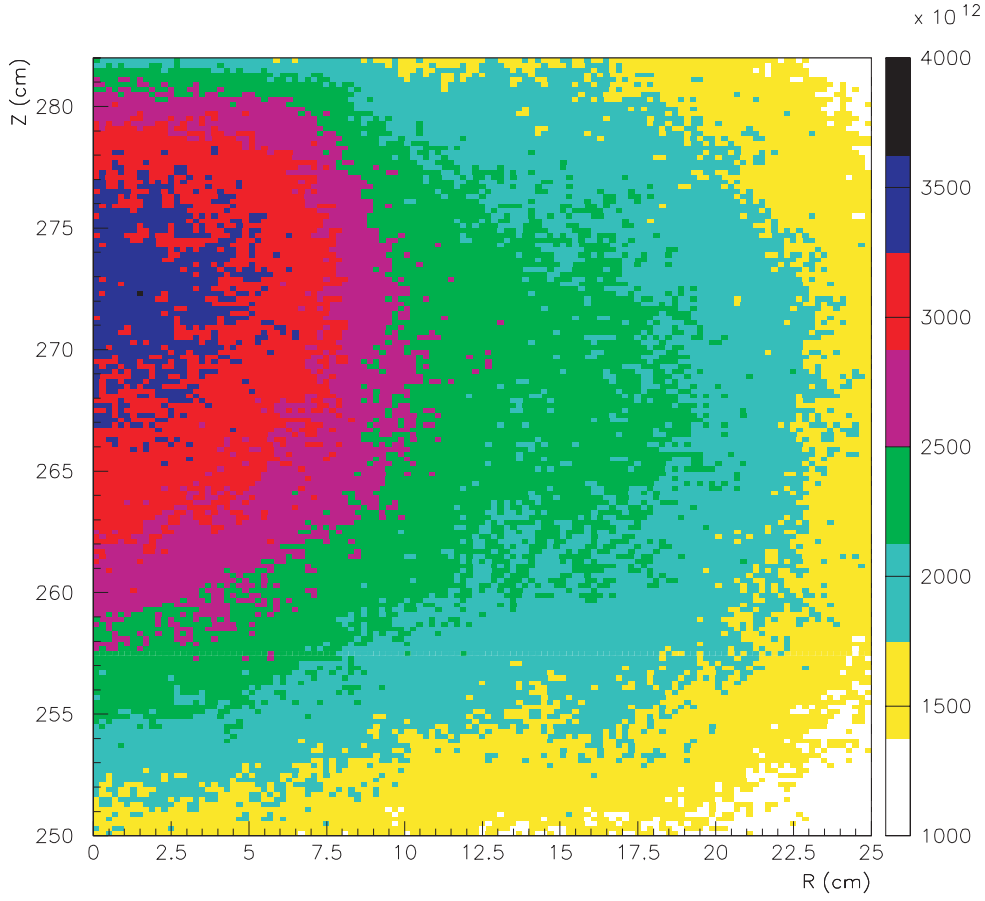

Figure 13. SCM-100 fast neutron flux (0.1 to 20 MeV) n/cm^2/s with the lead-bismuth target

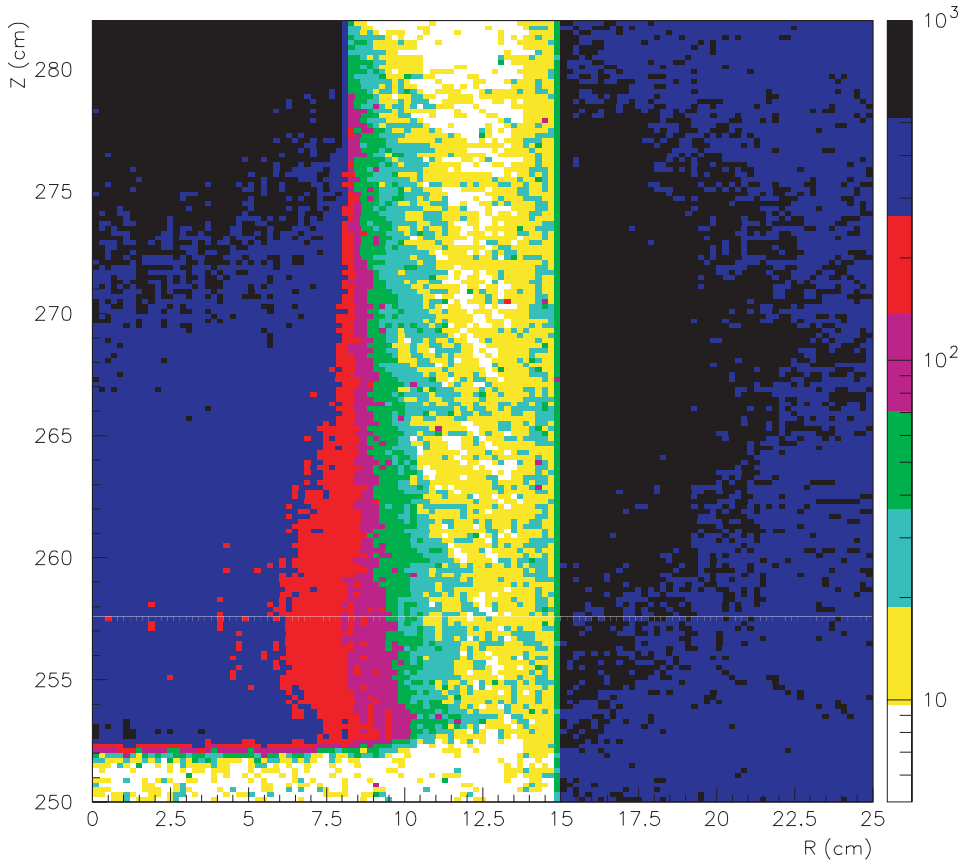

Figure 14. SCM-100 energy deposition distribution with the lead-bismuth target, W/cm^3

Table 1. Beam window nuclear responses

Energy deposition, W/cm^3	766.49
Atomic displacement, dpa/y	
Neutrons	46.2
Protons	21.1
Total	67.3
Helium production, appm/fpy	
Low energy neutrons ≤ 20 MeV	5.7
High energy neutrons > 20 MeV	50.2
Protons	1437.3
Total	1493.2
Hydrogen production, appm/fpy	
Low energy neutrons ≤ 20 MeV	6.3
High energy neutrons > 20 MeV	1010.1
Protons	26753.1
Total	27769.5

Table 2. Calculated stresses and HT-9 allowable stresses for the 3.5 mm beam window

Window Type		Conical Window			Hemi-Spherical Window		
Stress Component†	Allowable stress	Calculated Stress (MPa)	Allowable Stresses (MPa)	Temperature (C)	Calculated Stress (MPa)	Allowable Stresses (MPa)	Temperature (°C)
P_M	S_m	19.3	182*	277	23.6	182*	277
P_L+P_B	$K_{eff}\ S_m$	50.0	--**	277	24.3	--**	277
P_L+Q_L	S_e	74.0	182	433	56.9	182	417
P_L+P_B+Q+F	S_{d1}	434.9	--***	517	423.5	--***	500
P_L+P_B+Q	S_{d2}	396.9	363	517	374.2	386	500

* The allowable is calculated at the maximum temperature (433 C) to be on the conservative side since the S_m value is not available at 277 C

** Larger or equal to Sm

*** Larger than S_{d2}

†P_m : Primary membrane stress, P_L : Primary membrane stress plus additional local membrane stress, P_B :Primary bending stress, Q: Secondary stress, Q_L : Membrane part of the secondary stress, and F : Peak stress